TECHNICAL PAPER

ISSN 1047-3289 *J. Air & Waste Manage. Assoc.* **56**:961–976
Copyright 2006 Air & Waste Management Association

Transport and Dispersion during Wintertime Particulate Matter Episodes in the San Joaquin Valley, California

Clinton P. MacDonald, Michael C. McCarthy, Timothy S. Dye, Neil J.M. Wheeler, Hilary R. Hafner, and Paul T. Roberts
Sonoma Technology, Inc., Petaluma, CA

ABSTRACT

Data analysis and modeling were performed to characterize the spatial and temporal variability of wintertime transport and dispersion processes and the impact of these processes on particulate matter (PM) concentrations in the California San Joaquin Valley (SJV). Radar wind profiler (RWP) and radio acoustic sounding system (RASS) data collected from 18 sites throughout Central California were used to estimate hourly mixing heights for a 3-month period and to create case studies of high-resolution diagnostic wind fields, which were used for trajectory and dispersion analyses. Data analyses show that PM episodes were characterized by an upper-level ridge of high pressure that generally produced light winds through the entire depth of the atmospheric boundary layer and low mixing heights compared with nonepisode days. Peak daytime mixing heights during episodes were ~400 m above ground level (agl) compared with ~800 m agl during nonepisodes. These episode/nonepisode differences were observed throughout the SJV. Dispersion modeling indicates that the range of influence of primary PM emitted in major population centers within the SJV ranged from ~15 to 50 km. Trajectory analyses revealed that little intrabasin pollutant transport occurred among major population centers in the SJV; however, interbasin transport from the northern SJV and Sacramento regions into the San Francisco Bay Area (SFBA) was often observed. In addition, this analysis demonstrates the usefulness of integrating RWP/RASS measurements into data analyses and modeling to improve the understanding of meteorological processes that impact pollution, such as aloft transport and boundary layer evolution.

INTRODUCTION

In the California San Joaquin Valley (SJV), the concentrations of particulate matter (PM) with diameters of <2.5 μm ($PM_{2.5}$) often exceed the National Ambient Air Quality Standards; the highest concentrations are typically observed during fall and winter.[1–3] The San Joaquin Valleywide Air Pollution Study Agency sponsored the California Regional $PM_{10}/PM_{2.5}$ Air Quality Study (CRPAQS) to investigate the causes of high $PM_{2.5}$ concentrations and to provide information to design effective PM control strategies in the SJV. The CRPAQS field campaign was conducted from December 1, 1999, through February 3, 2001. The spatial and temporal variability of transport and dispersion processes in the SJV during the CRPAQS winter episode are presented in this paper.

Research to investigate air pollution issues in the SJV has typically been conducted for summer and focused on O_3.[4–6] A limited number of studies have focused on wintertime PM,[7] most notably the 1995 Integrated Monitoring Study (IMS95).[8–10] During summer, onshore winds dominate flow across the San Francisco Bay Area (SFBA), SJV, and Sacramento Valley. The onshore flow moves across the SFBA before diverging over the Sacramento River Delta; a northerly component moves through the Sacramento Valley and a southerly component through the SJV.[11] Many studies have shown that transport of O_3 and O_3 precursors from the SFBA impact the air quality in the SJV.[5,6,12–14]

Conversely, winter conditions are typically characterized by light offshore flow.[11] However, there are periods of light and variable winds and strong stability when the most extreme PM episodes occur. The stagnation periods are interrupted by storms impacting the West Coast that produce moderate-to-strong winds and a deep boundary layer, which effectively disperse pollutants accumulated during the stagnation periods.

Research on wintertime PM in the SJV is limited, and numerous questions about transport and dispersion processes of PM and its precursors remain unanswered. In this paper the authors address the following questions: (1) Does interbasin (between basin) or intrabasin (within a basin) transport of pollutants occur during wintertime PM episodes?; (2) What is the relationship between synoptic- and regional-scale meteorological conditions and interbasin and intrabasin wintertime transport?; (3) How are primary particles generated in urban areas transported to nonurban or "downwind" urban areas under low wind speed/stagnant conditions?; (4) Do nocturnal jets and eddy circulations occur during wintertime PM episodes, and do they play a role in dispersing material throughout the SJV?; and (5) How does the diurnal evolution of boundary layer height (e.g., mixing height), winds, and ventilation vary during episodes and nonepisodes and in

IMPLICATIONS

Wintertime pollutant transport into the SJV from surrounding areas is not a significant contributor to PM in the SJV. Moreover, there is evidence of transport from the SJV and Sacramento regions into the SFBA. The lack of transport into the SJV suggests that emission controls within the SJV will be most effective in reducing PM concentrations in the SJV.

different regions of the SJV? The answers to these questions contribute to the overall conceptual model that explains the chemical, emission, and meteorological processes that influence wintertime PM concentrations in the SJV.[15]

EXPERIMENTAL WORK

Describing the transport and dispersion processes impacting PM in the SJV requires multiple data analysis techniques and a variety of measurements from numerous sites. The data analysis techniques used in this study include statistical analysis, case study analysis, meteorological and dispersion modeling, and trajectory analysis.

Data

The data used in the analyses included PM measured with continuous $PM_{2.5}$ β attenuation monitors (BAMs), estimated from nephelometer data using a technique suggested by Richards et al.[16] and Alcorn et al.[17] and measured using 24-hr filters. Although both $PM_{2.5}$ and coarse PM (PM_{10}) are of concern, $PM_{2.5}$ data were the focus of these analyses, because $PM_{2.5}$ contributes most to PM_{10} mass during winter episodes.[18] In addition, the data included the major chemical components of PM measured on 24-hr filters, such as ammonium, nitrate, and organic material (OM). The surface meteorological data included hourly wind speed, wind direction, temperature, relative humidity, and pressure from 359 federal, state, and local agency monitors (Figure 1a). The upper-air data consisted of 915-MHz radar wind profiler (RWP)/radio acoustic sounding system (RASS)-derived vertical profiles of hourly horizontal wind and virtual temperature (T_v) data collected from 18 sites and twice daily (12:00 a.m. and 12:00 p.m. Greenwich Mean Time) rawinsonde data collected from five sites. The height coverage of the horizontal winds derived by the RWP network is up to ~4000 m above ground level (agl) with a vertical resolution of ~100 m. The T_v measurements derived using RASS measurements had height coverage up to ~1500 m agl with a vertical resolution of ~60 m.

RWP, RASS, and surface meteorological measurements were used to obtain estimates of mixing height and boundary layer wind speed and to compute ventilation index. The ventilation index (m^2/sec) provides a measure of the dispersion potential of the atmosphere for pollutants and is the product of mixing height (m agl) and boundary layer wind speed (m/sec).

Daytime mixing heights were determined with an automated method that used T_v measurements derived by RASS in a stability analysis. Nighttime mixing heights were determined with an algorithm that evaluates the continuity of T_v on an hourly basis at each sample height between the current hour and previous hour to determine the extent of mixing from the surface. A more detailed description of the mixing height algorithms used to generate hourly estimates of mixing height for CRPAQS is described below. Mean boundary layer wind speed was derived using RWP measurements at heights between 180 and 320 m. This height range was chosen to obtain a reasonable estimate of winds within the atmospheric boundary layer (ABL). However, it should be noted that during the night, these levels are often above the top of the nocturnal boundary layer (NBL), and wind speeds may be greater than wind speeds within the NBL.

Statistical Analysis

Statistical analyses were performed to understand the difference in mixing height, boundary layer winds, and ventilation between episode and nonepisode days from November 1, 2000, through January 31, 2001. For this and several other analyses, the SJV was divided into three subregions: northern valley (NV), mid-valley (MV), and southern valley ([SV] Figure 1b). Major cities in these subregions are Modesto (M14) and Stockton in the NV, Fresno (FSF) in the MV, and Bakersfield (BAC) in the SV (Figure 1c).

For each subregion, the meteorological measurements, air quality measurements, and a number of derived quantities (e.g., mean boundary layer wind speed and ventilation index) were grouped and averaged by hour according to two classification schemes: (1) episode and nonepisode days defined by the daily maximum $PM_{2.5}$ concentration, and (2) upper-air synoptic weather pattern. A single day in each of the three subregions was classified as an episode day if the 24-hr average $PM_{2.5}$ concentration exceeded 40 $\mu g/m^3$, which is the threshold $PM_{2.5}$ value representing the Unhealthy for Sensitive Groups category on the Air Quality Index. Because episode days are typically characterized by an upper-level ridge of high pressure, and nonepisode days are typically characterized by an upper-level trough of low pressure, the two classification schemes produced similar results; therefore, statistical analyses presented in the following sections focus on the episode/nonepisode classification scheme. However, significant results from the meteorological classification are also presented. The similarity in the results between the two classification schemes reinforces the relationship among synoptic-scale meteorology, local meteorology, and air quality.

Case Study Analysis

Case study analyses were performed for two intensive operations periods (December 25–30, 2000, and January 3–8, 2001) to augment the statistical analyses. The case study analyses incorporated meteorological and dispersion modeling, as well as a trajectory analysis, using the CALMET meteorological model[19] and the CALPUFF dispersion model.[20] The air quality monitoring sites selected for analysis consisted of one site from each subregion of the SJV: M14 in the NV, FSF in the MV, and BAC in the SV (Figure 1c). In addition, continuous $PM_{2.5}$ measurements from the Angiola (ANGI) air monitoring site were analyzed, because it is in a more rural location compared with the other three monitoring sites. The air quality monitoring sites were selected for their locations in the subregions of interest and the continuous $PM_{2.5}$ measurements recorded at each site ($PM_{2.5}$ BAM measurements at all sites except M14, where only nephelometer measurements were available). Comparisons between the mean episode metrics and case study period metrics were also performed to determine whether the case study periods were representative of the episode days.

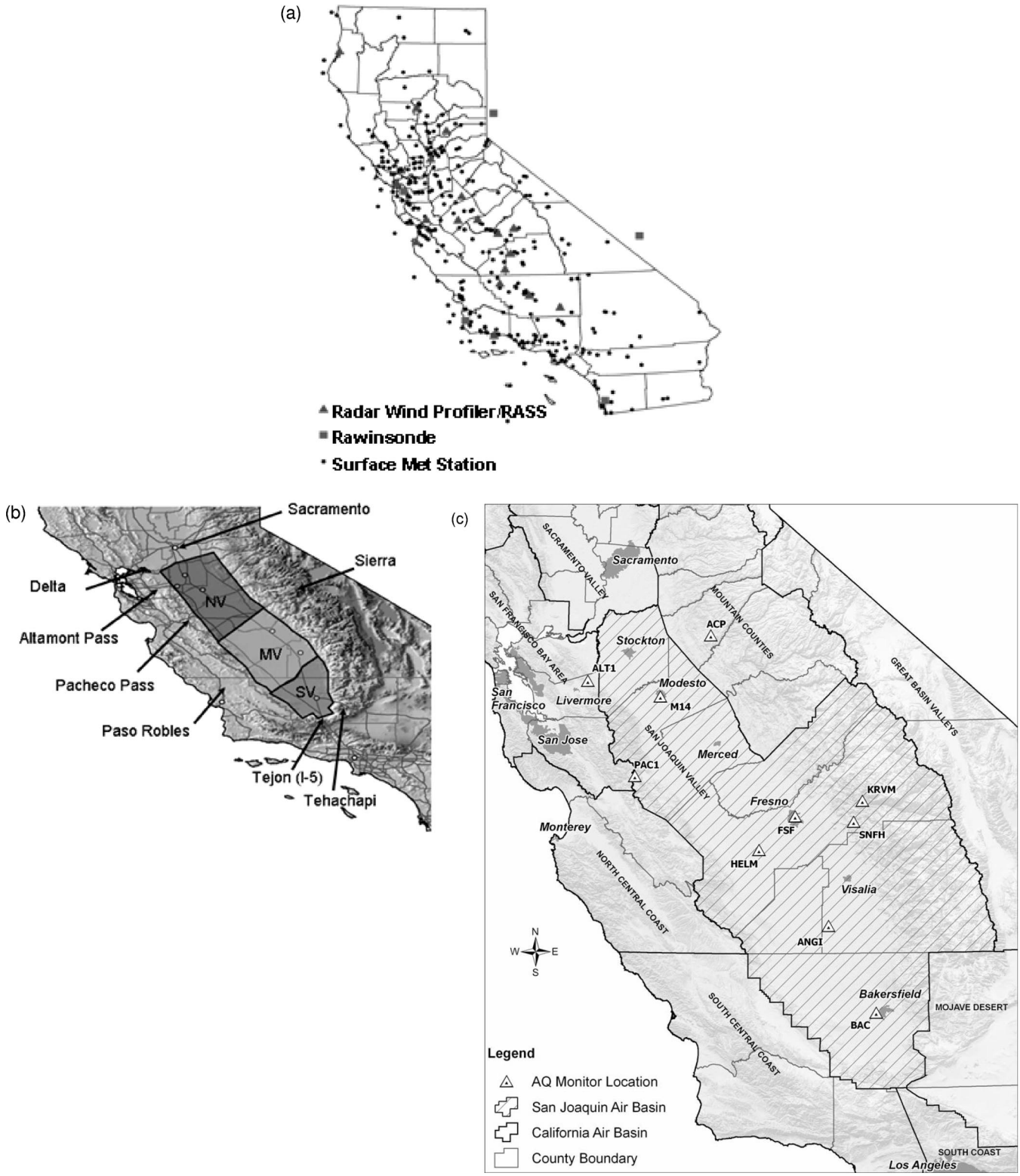

Figure 1. Maps of (a) meteorological measurement locations, (b) subregions of the SJV and potential transport pathways, and (c) air quality sites and cities referenced in this paper.

Meteorological Modeling

The CALMET model combines objective and diagnostic analysis methods to generate three-dimensional meteorological fields through integration of meteorological data (surface and upper-air measurements) and geophysical data (terrain and land use data). The CALMET model produces gridded meteorological fields of three-dimensional winds, air temperature, and other turbulence and stability fields.[19] The CALMET model includes a diagnostic wind-field generator containing objective analysis and parameterization treatments of slope flows, kinematic terrain effects, terrain-blocking effects, a divergence minimization procedure, and a micrometeorological model for overland and overwater boundary layers.[19] The CALMET model was used to resolve mesoscale and local-scale meteorological phenomena through blending observational meteorological data with synoptic-scale meteorological model results and analyses.

The CALMET modeling domain used in this analysis was a 1092-km × 1092-km area covering the state of California. The horizontal grid resolution was 4 km throughout the domain. The model contained 20 vertical layers from the surface to 2750 m agl, with higher resolution near the surface and lower resolution in the upper-levels. The horizontal and vertical resolution was chosen to capture and resolve the timing, strength, and vertical structure of important atmospheric processes within the surface layer (SL) and boundary layer, especially those processes impacting the transport and diffusion of chemical species during wintertime episodes in the SJV.

This modeling domain consisted of a variety of distinctly different microclimates and widely varying landscapes exemplified by the Sierra Nevada Mountain Range, the Coastal Range, the central SJV, Death Valley, and the Pacific coastline. The elevation range within the modeling domain included Mount Whitney, with an elevation of 4418 m (14,494 ft), and Death Valley, which lies nearly 86 m (282 ft) below sea level. The highly variable landscape within the modeling domain created the potential for significant terrain influence on wind flows, as well as other meteorological output fields. The physics embedded within the CALMET meteorological model enabled the influence of terrain on atmospheric properties to be captured and modeled.

The data used in the CALMET model included the surface and aloft meteorological measurements and the Eta Data Assimilation System (EDAS) model output. The EDAS data are constructed from successive 3-hr Eta model forecasts.[21] The Eta model is a regional-scale meteorological forecast model applied with 40-km horizontal resolution and 26 vertical levels (every 25 mb up to 850 mb, then every 50 mb up to 50 mb). The advantage of using EDAS data for the initial field is its highly resolved temporal and spatial information,[22] as compared with the domain mean wind field typically derived from twice daily soundings.

The CALMET modeling procedure is composed of several steps. First, an objective combination of the 3-hr EDAS analyses and the surface and upper-air observations was performed using three-dimensional weighting factors for each 4-km CALMET grid cell. The weighting factors were created using the distance from each grid cell to an observation, the height of the CALMET layer compared with the observation height, and the slope of the terrain. The weighting factors were designed to increase the influence of measured data at CALMET grid cells "close" to the measurement sites and to increase the influence of EDAS model output for grid cells "far" from the measurement sites. Thus, the resulting CALMET winds resolve observed features, such as a low-level jet if such features are observed by RWPs. The objectively combined data produced a gridded wind field, which was then smoothed and adjusted for terrain before producing a "final" wind field. In the process described above, both the EDAS model output and the observational data have been subjected to the terrain blocking and slope flow schemes of CALMET. Typically, interpolated observations are not subjected to the terrain-blocking schemes. Figure 2 illustrates the distinctly differing surface wind fields that result when observational data are not subjected to the terrain-blocking and slope-flow schemes of CALMET (Figure 2a) in comparison with wind fields that result when both the EDAS model output and observational data are subjected to the terrain-blocking and slope-flow schemes of CALMET (Figure 2b). Winds highlighted by the rectangle in Figure 2a are not influenced by the terrain and unrealistically flow through the mountainous terrain, whereas winds in Figure 2b converge in canyons and flow around the mountains.

Dispersion Modeling

The CALPUFF model is a multilayer, multispecies, non-steady-state puff dispersion model that simulates the effects of time- and space-varying meteorological conditions on pollutant transport and removal. The three-dimensional meteorological fields derived by the CALMET model were used in the CALPUFF model to evaluate the impact of dispersive and diffusive processes on primary pollutants within the SJV during the case study periods, December 25–30, 2000, and January 3–8, 2001. An emission rate of 31 t/day was used to represent the primary $PM_{2.5}$ emissions for Fresno County, the largest population center in the SJV.[23] The emission rates for the next three largest population centers within the SJV (BAC, Stockton, and M14) and for Sacramento were scaled by the ratio of each population center to the population of FSF. Multiple tracers were used to identify the extent of the impact of emissions from each location on surrounding areas. The simulations were not intended to predict absolute concentrations but to identify relative concentrations among case study days and subregions. For example, this analysis could identify the relative source contributions to primary PM in the rural areas within the SJV. The emission rates represent primary emission sources, and the simulations do not account for secondary formation of $PM_{2.5}$ or deposition. CALPUFF simulations were run continuously from the beginning of each episode. The range of emissions was quantified by analyzing the maximum distance to which predicted concentrations were approximately one tenth of the maximum predicted urban concentration (~50 $\mu g/m^3$). Table 1 summarizes the emission range and movement of the plume for the January 2001 study period.

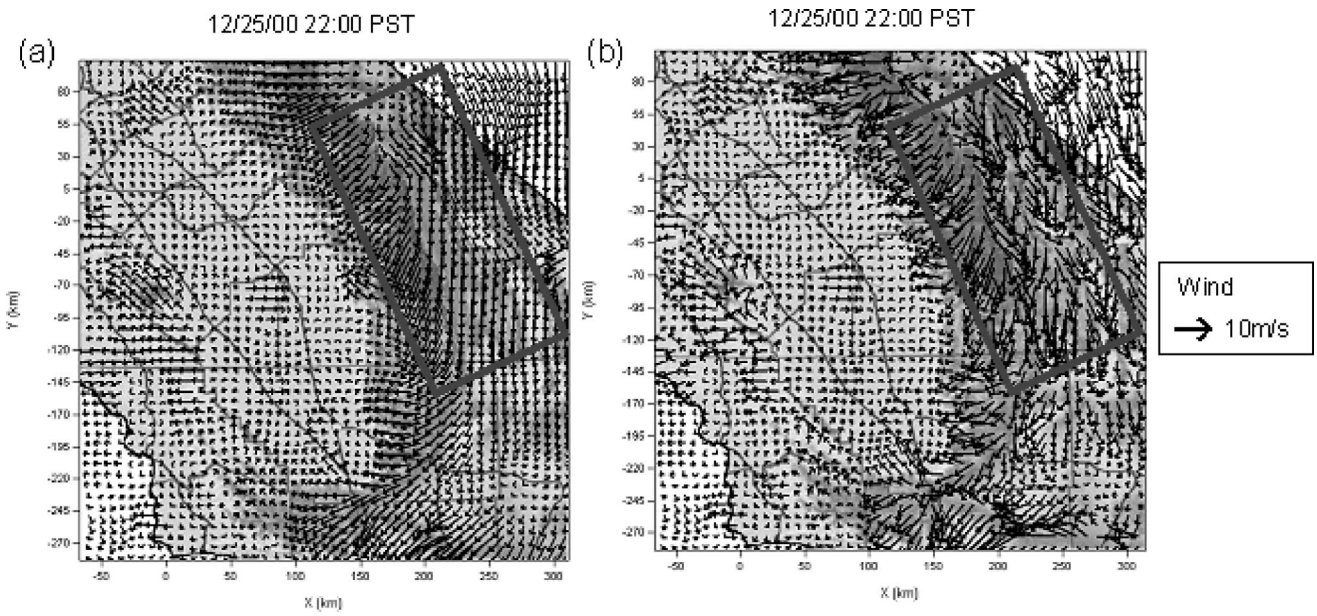

Figure 2. CALMET surface wind fields when (a) observational data are not subjected to the CALMET terrain adjustment procedure and (b) observational data are subjected the CALMET terrain adjustment procedure. Boxes show areas of high terrain elevation.

Trajectory Analysis

To characterize the transport of pollutants throughout the SJV and surrounding basins, 24-hr backward and forward trajectories were calculated using the three-dimensional winds derived by the CALMET model. The trajectories were calculated for the following locations: ANGI, Sierra Nevada Foothills (SNFH), BAC, FSF, San Jose, San Francisco, Monterey, Sacramento, and Stockton (Figure 1c). The trajectories were calculated twice daily, at 6:00 a.m. and 3:00 p.m. Pacific Standard Time (PST), to evaluate diurnal differences in transport in and around these locations. Finally, the trajectories were calculated at 35 and 450 m agl to capture the transport difference between the surface and the boundary layer.

Subjective analysis of the trajectories consisted of identifying frequent transport pathways that result in the exchange of air between the SJV and areas outside the SJV. Table 2 summarizes the frequency at which forward trajectories, originating from various sites and heights, flowed through various pathways in and around the SJV.

Estimating Mixing Heights

The ABL is the portion of the earth's atmosphere that is directly influenced by the physical characteristics of the surface (terrain) and surface processes, such as friction, heating and cooling, and chemical emissions.[24,25] In nonmarine environments, the ABL comprises the SL, convective boundary layer (CBL), NBL, residual layer, and the

Table 1. Summary of arbitrary emission plume range of influence (km) and dominant direction from five population centers in California using CALPUFF dispersion modeling for the January 2001 case study period.

Δt	Date and Time (PST)	Sacramento	Stockton	M14	FSF	BAC
6	1/3/01 6:00 a.m.	60	25	15	25	15
15	1/3/01 3:00 p.m.	50	25	10	30	25
30	1/4/01 6:00 a.m.	50 (West)	40	25	40	30
39	1/4/01 3:00 p.m.	60 (West)	20	15	40	25
54	1/5/01 6:00 a.m.	50	25	15	40	30
63	1/5/01 3:00 p.m.	100 (West)	15	10	30	30
78	1/6/01 6:00 a.m.	85 (North)	60 (North)	5	50 (North)	30 (North)
87	1/6/01 3:00 p.m.	60 (West)	25	5	25	20
102	1/7/01 6:00 a.m.	50 (West)	25	30	50 (North)	25
111	1/7/01 3:00 p.m.	35	ND[a]	ND[a]	200 (North)	25
126	1/8/01 6:00 a.m.	50 (North)	ND[a]	ND[a]	60 (North)	20
135	1/8/01 3:00 p.m.	15	ND[a]	ND[a]	15	25
Min	1/3/01 to 1/8/01	15	ND[a]	ND[a]	15	15
Max	1/3/01 to 1/8/01	100	60	30	200	30
Mean	1/3/01 to 1/8/01	55	29	14	50	25

Note: CALPUFF simulation was run from the beginning of the episode, and the area of influence of the emission plumes was quantified by analyzing the maximum distance to which predicted concentrations were approximately one tenth of the maximum predicted urban concentration (50 $\mu g/m^3$) in the case study period.
[a]ND = concentrations > 5 $\mu g/m^3$ not detected.

Table 2. Number of occurrences (of 19 possible) within the December 2000 and January 2001 case study periods where forward trajectories (6:00 a.m. and 3:00 p.m. PST), originating from various sites and at two heights (35 and 450 m agl), used various pathways in and around the SJV.

	Sites/Height											
	Stockton		FSF		BAC		Sacramento		San Francisco		San Jose	
Pathways (see Figure 1b)	35 m	450 m	35 m	450 m	35 m	450 m	35 m	450 m	35 m	450 m	35 m	450 m
Δ	13	6	0	0	0	0	10	9	0	0	0	0
ALT1	1	5	0	0	0	0	0	2	0	0	0	5
PAC1	0	3	0	0	0	0	0	0	0	0	0	0
Paso Robles	0	0	0	0	0	0	0	0	0	0	0	0
Tejon (I-5)	0	0	0	0	0	2	0	0	0	0	0	0
Tehachapi	0	0	0	0	0	0	0	0	0	0	0	0
Sierra	0	0	1	3	0	0	0	0	0	0	0	0
Sacramento	0	1	1	3	0	0	0	0	0	0	0	0

entrainment zone (EZ). The height of these layers influences atmospheric dispersion, accumulation, and dilution of pollutants.[26,27]

The processes by which the daytime CBL and the NBL evolve are different. The CBL evolves because of strong buoyant vertical motions and mechanical turbulence. The statically stable NBL evolves because of radiational cooling of the surface and mechanical turbulence that slowly and sporadically mixes cool surface air vertically.

Mixing heights were computed at 18 RASS sites from November 15, 2000, through January 31, 2001. The typical resolution of the RASS T_v measurements was ~60 m; the lowest sampling height was near 120 m agl and a maximum sampling height near 1500 m agl. Temperature measurements at the surface (2 m) were converted to T_v and merged with the RASS measurements to provide information about the stability profile in the SL and near-surface layer.

Daytime mixing heights were estimated using T_v measurements by analyzing stability at each sampling height to detect an increase in temperature denoting the top of the CBL. The algorithm accounted for lapse rate differences caused by both saturated and unsaturated atmospheric conditions. The T_v profiles generally detected the height of the CBL; however, on a few occasions, the height of the CBL exceeded the maximum sampling height of the RASS measurements.

Nighttime mixing heights were estimated by evaluating the temporal continuity of RASS T_v profiles to determine the vertical extent to which cool surface air mixed from 1 hr to the next. The height to which the cool surface air had mixed was the estimate of mixing height. This method accounted for the hour to hour fluctuations in the height of the NBL, ignoring temperature advection and assuming that the surface continually cooled throughout the night. All of the mixing heights were subjectively quality controlled for meteorological reasonableness.

Spatial Analysis

Wintertime $PM_{2.5}$ in the SJV was composed of a number of chemically distinct components. Ammonium nitrate and OM typically accounted for >80% of the measured $PM_{2.5}$ mass during winter episode days. Concentrations of ammonium nitrate were calculated as $1.29 \times NO_3^-$ filter measurements. Concentrations of OM were calculated as 1.4×organic compounds (OCs). OM concentrations are dominated by primary emissions,[28] whereas the ammonium nitrate is formed in the atmosphere (i.e., secondary formation). Ambient measurements of ammonium nitrate and OM from 24-hr filters during the winter episode days from all of the CRPAQS sites were plotted on maps to examine spatial patterns in primary and secondary pollutants in relation to meteorology.

Pollution Roses

Wind and pollution roses were created for four interbasin transport sites in the SJV for the winter 2000 and 2001 episode (i.e., December 14, 2000, to January 7, 2001). Wind roses were generated using 10-m tower meteorological data. Pollution roses were generated using wind directions from the same meteorological data and surface nephelometer or BAM measurements. Roses were split among morning, afternoon, and evening times.

RESULTS

Statistical Analysis

Air Quality and Meteorological Summary. The episode and nonepisode days for each subregion of the SJV were classified based on the 40-μg/m^3 daily maximum $PM_{2.5}$ concentration criterion. The number of episode days exceeded the number of nonepisode days in the MV and SV (53 and 39 and 67 and 24, respectively), whereas in the NV, the number of episode days occurred less frequently than nonepisode days (22 and 34). The smaller number of episode days in the NV is caused by the combination of local meteorology (increased mixing height and winds) and lower $PM_{2.5}$ emissions[29] compared with the MV and SV. The NV had a lower number of total days with available data compared with other subregions. However, a review of air quality in nearby subregions indicated that the missing days of data in the NV would not likely skew the observed episode/nonepisode day ratio.

Classifications of the daily synoptic weather patterns combined with $PM_{2.5}$ episode information show that episode days were dominated by a strong upper-level ridge

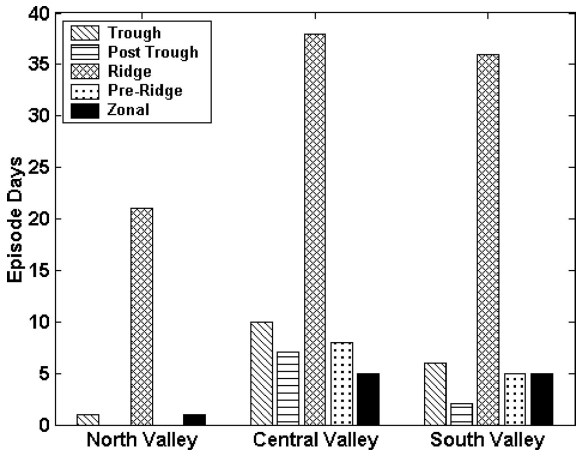

Figure 3. The frequency of episode days in the SJV by subregion and synoptic classification from November 15, 2000, through January 31, 2001.

of high pressure located over Central California. In particular, the ridge pattern (ridge and preridge), characterized by light winds, low mixing heights, and limited dispersion of pollutants throughout the SJV, dominated episode days in the NV, MV, and SV, making up more than two thirds of the episode days (Figure 3). Conversely, an upper-level trough of low pressure and an associated cold front typically caused stronger winds and higher mixing heights that enabled effective horizontal and vertical dispersion of pollutants in the SJV, resulting in lower pollutant concentrations. Trough patterns (trough and post-trough) dominated nonepisode days in the NV, MV, and SV, comprising three fourths of the nonepisode days. Although the ridge pattern dominated on episode days and the trough pattern on nonepisode days, a few days do not fit these classifications. Pollution was not always effectively removed from the SJV after a trough and frontal passage, because occasionally the dynamics associated with a trough were not strong enough to disperse the pollutants accumulated in the SJV. Conversely, after the onset of a ridge, 1 or 2 days were sometimes needed for $PM_{2.5}$ concentrations to accumulate before exceeding the 40 $\mu g/m^3$ criterion.

Meteorological Conditions on Episode and Nonepisode Days. Mean daytime hourly mixing heights were lower on episode days than on nonepisode days from ~9:00 a.m. to 5:00 p.m. PST for all of the subregions of the SJV (Figure 4). In addition, the peak afternoon mixing heights, which occurred between 2:00 p.m. and 3:00 p.m. PST, were approximately 1.5–2.0 times lower on episode days than on nonepisode days. The mixing height growth rate from 8:00 a.m. to 3:00 p.m. PST was half as fast on episode days compared with nonepisode days. On episode days, the mean maximum mixing height ranged from 368 to 518 m agl. During nonepisode days, the mean maximum mixing height ranged from 745 to 910 m agl. Nighttime mixing heights for both episode and nonepisode days were similar throughout each subregion of the SJV and were ~50–100 m agl. Historical winter daytime mixing height estimates in the SJV typically ranged from 500 to 1000 m agl.[1,6,27,30]

Mean boundary layer wind speeds were lower on episode days (2–3 m/sec) than on nonepisode days (4–6 m/sec) throughout the SJV. There was also less diurnal variability in mean wind speeds on episode days compared with nonepisode days. Wind speeds on nonepisode days were lowest in the late afternoon and evening, almost decreasing to the mean wind speeds of episode days.

The peak ventilation index was 2.5–4.0 times greater on nonepisode days than on episode days (Figure 5). This is a direct result of lower mixing heights and lower wind speeds typically present on episode days. The diurnal

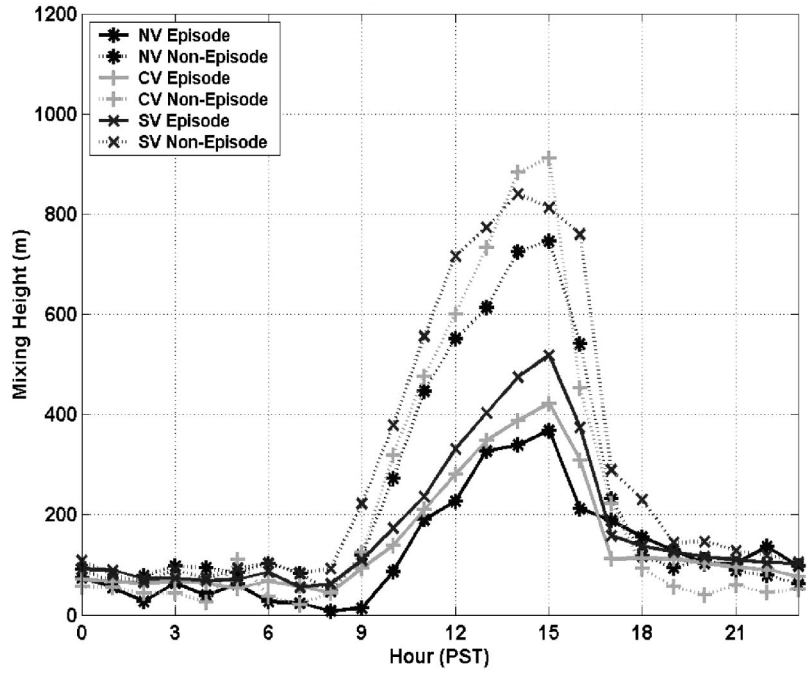

Figure 4. Mean diurnal mixing heights on episode and nonepisode days by subregion from November 15, 2000, through January 31, 2001.

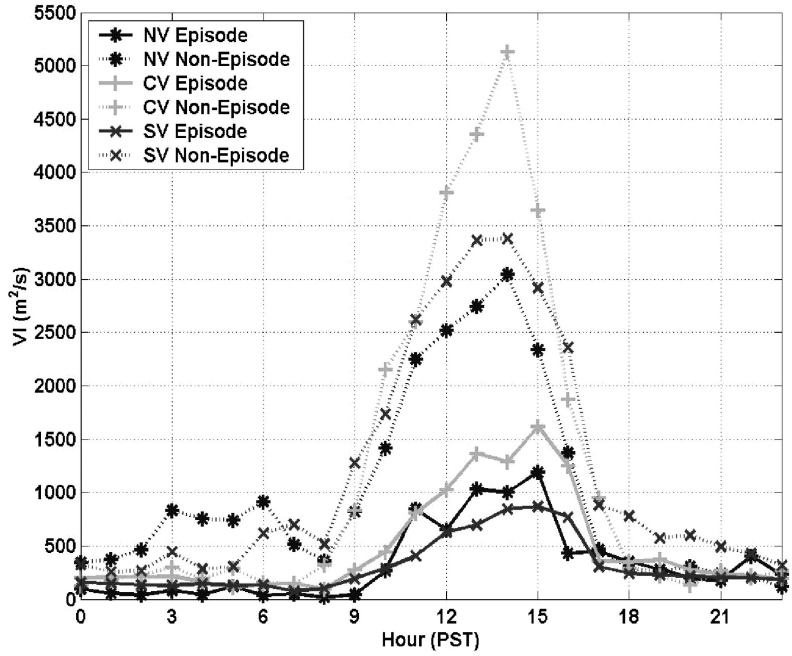

Figure 5. Mean diurnal ventilation index on episode and nonepisode days by subregion from November 15, 2000, through January 31, 2001.

cycle in the ventilation index closely follows the diurnal cycle in mixing height. Peak ventilation occurred between 2:00 p.m. and 3:00 p.m. PST, coinciding with the peak afternoon mixing height. On episode days, the MV exhibited the highest average ventilation index (1600 m^2/sec) compared with the NV (1200 m^2/sec) and the SV (850 m^2/sec). On nonepisode days, the greatest mean ventilation index was also observed in the MV (5100 m^2/sec), whereas the ventilation index in the NV and SV was considerably lower but still much greater than on episode days (NV, 3000 m^2/sec and SV, 3400 m^2/sec). In summary, mean meteorological metrics (mixing height, mean boundary layer wind speed, and ventilation index) were distinctly different for episode and nonepisode days; however, it should be noted that there is day-to-day variation within each category.

Case Study Analysis

The case study analysis of the $PM_{2.5}$ episode from December 25, 2000, through January 8, 2001, provides a description of the general air quality and meteorological conditions present in the SJV, a comparison of the meteorological metrics observed during the case study and mean meteorological metrics calculated on episode days, and a description of the meteorological and dispersion modeling and trajectory analysis.

General Meteorology. The synoptic-scale meteorological conditions underwent little change throughout the December 2000 and January 2001 episode. Aloft, a large upper-level ridge of high pressure remained nearly stationary over the West Coast, resulting in increased stability, low afternoon mixing heights, and light winds throughout the entire depth of the boundary layer. At the surface, a strong surface high-pressure system remained centered over the Intermountain West. These conditions resulted in generally calm to light offshore winds. The low mixing heights and light winds limited the dispersion of $PM_{2.5}$, allowing $PM_{2.5}$ to accumulate in the SJV throughout both periods. On January 8, 2001, a strong upper-level trough of low pressure and associated cold front moved across Central California. A clean air mass moving onshore with this system, combined with increased winds and higher mixing heights, caused $PM_{2.5}$ concentrations to decrease to <35 $\mu g/m^3$ in urban locations and to <10 $\mu g/m^3$ in rural locations. Despite the similarities between the two case study periods, fog was more common during the December episode as measured at ANGI (see Figure 1c). During the December episode, fog was reported on December 25, 27, 28, and 31, whereas, during the January episode, fog occurred on January 6 and 8 and only during the morning hours.

General Air Quality. $PM_{2.5}$ concentrations increased throughout the December 25, 2000, through January 7, 2001, time period at most sites. The highest concentrations were observed on January 1 in FSF, BAC, and Sacramento; concentrations at rural SV sites peaked on January 5 or 6, and concentrations at sites north of Pacheco Pass (PAC1) peaked on January 6 or 7. In addition to the days mentioned above, high concentrations were observed on many other days during this episode.

The spatial distribution of $PM_{2.5}$ concentrations illustrates the regional nature of winter PM pollution within the topographic boundaries of the SJV. $PM_{2.5}$ concentrations were highest at urban sites in FSF and BAC. Concentrations were lower at elevated sites to the east and west of the SJV (e.g., at Angel's Camp [ACP] and SNFH in the Sierra and at PAC1 in the coastal range) than in the SJV itself. Elevated sites (400–1000 mean sea level) on the eastern, southern, and western borders recorded $PM_{2.5}$ concentrations significantly lower than those in the SJV; this difference suggests that the high $PM_{2.5}$ concentrations were limited to the first 300–500 m above sea level

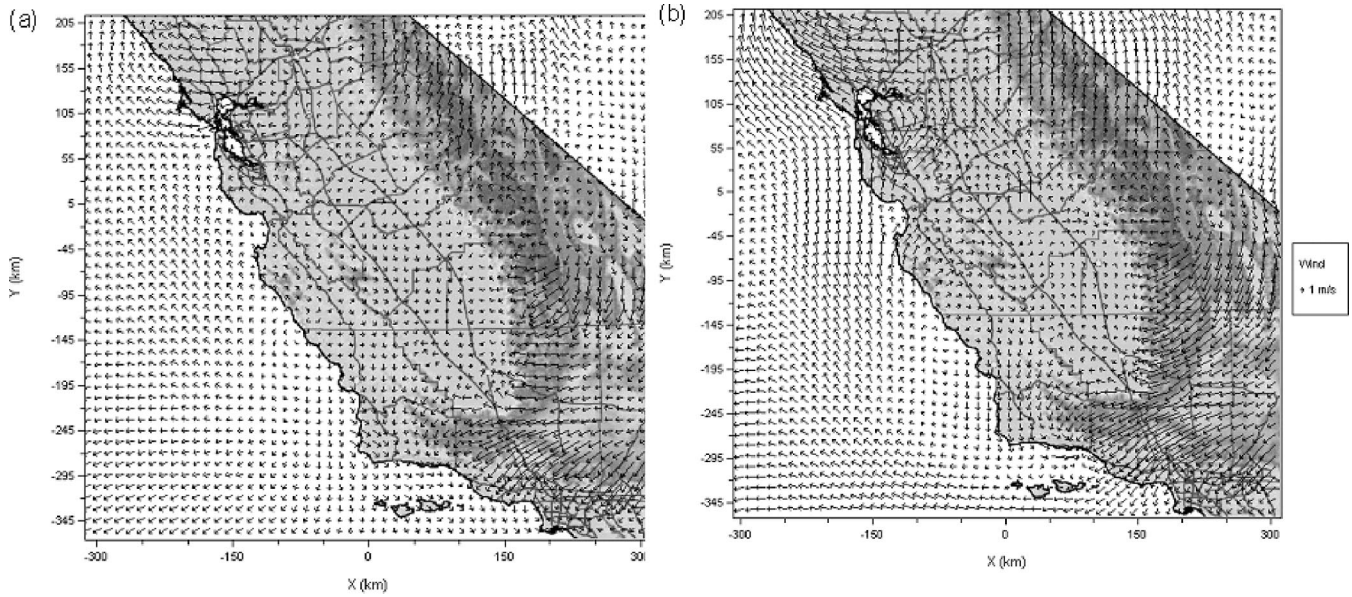

Figure 6. (a) CALMET wind fields at 35 m agl and (b) CALMET wind fields at 450 m agl, December 26, 2000, at 3:00 p.m. PST.

for most of the episode and that the $PM_{2.5}$ concentrations in air potentially flowing into the SJV were much lower than those within the SJV. This observation is consistent with the low mixing heights during episodes.

Case Studies Compared with Overall Statistics. Mixing heights during the case study periods were approximately the same as mean mixing heights calculated for all of the episode days from November 15, 2000, through January 31, 2001. Boundary layer winds during the case study period were somewhat lighter than the mean boundary layer winds on all of the episode days. These lighter boundary layer winds during the case study period subsequently resulted in lower ventilation index calculations.

Modeled Winds. Light and variable winds prevailed in the SJV during the episode. Typically, the light winds occurred throughout the depth of the boundary layer. Figure 6 depicts the CALMET wind fields and illustrates the spatial pattern of the light and variable winds in the SJV near the surface (35 m agl) and aloft (450 m agl) on December 26, 2000, at 3:00 p.m. PST. As discussed earlier, the synoptic-scale meteorological pattern was similar throughout the case study period, resulting in similar winds within each subregion of the SJV. However, a difference in the winds was noticeable among the SJV subregions, as expected, probably caused by mesoscale circulations and terrain-induced flows throughout the SJV.

Each of the three subregions of the SJV experienced light and variable winds. In the SV, winds were occasionally influenced by strong drainage flow out of the Sierra Nevada Mountains. The NV experienced instances of offshore flow at 35 and 450 m agl. As the strong low pressure system and associated frontal boundary approached the region toward the end of the January 2000 case study period (January 6, 2001), winds near the surface and aloft began to increase from the south throughout the entire SJV. Once the frontal boundary passed through the region, northwesterly winds were present in the SJV.

Vertical profiles of the horizontal wind from four RWPs (at BAC, Los Banos, Trimmer, and Waterford) in the SJV were analyzed for evidence of a wintertime nocturnal jet during the two case studies. This analysis yielded no evidence of a wintertime low-level nocturnal jet in the SJV. A representative example is shown in Figure 7. This time-height cross section of winds at Los Banos on December 28, 2000, shows light winds the entire day and night from the surface to ~400 m agl, light northerly winds >400 m, and no nocturnal jet. Typically, during the summertime, when a nocturnal jet occurs in the SJV, it is observed in the western SJV, including over Los Banos. Although a jet was not observed, enhanced winds associated with synoptic-scale phenomena (e.g., low pressure systems) were observed.

Modeled Trajectory Analysis. Table 1 summarizes the interbasin and intrabasin transport analysis in the SJV. Multiday CALMET-derived forward trajectories at heights of 35 and 450 m agl (Figures 8 and 9) were used to analyze transport pathways (Figure 1b) in and around the SJV.

Little evidence of intrabasin transport between FSF and BAC or FSF and Stockton/M14 exists. A single exception occurred near the end of the January 2001 episode as southerly winds increased because of an approaching frontal system. The approaching frontal system caused the forward trajectories originating at FSF to reach Sacramento and the Sierra Nevada Mountains (Figures 8b and 9b). During both case study periods at 450 m agl, evidence suggests possible transport from the BAC area through Tejon Pass (U.S. Interstate 5) to the Mojave Desert and Los Angeles Basin as shown in Figure 9.

Conversely, interbasin transport occurred frequently from the NV through the SFBA to offshore regions throughout both case studies. Forward trajectories originating in Sacramento and Stockton regularly traveled across the delta and exited through the SFBA (Figures 8 and 9). In addition, evidence suggests pollutant transport from Stockton and Sacramento exiting through Altamont

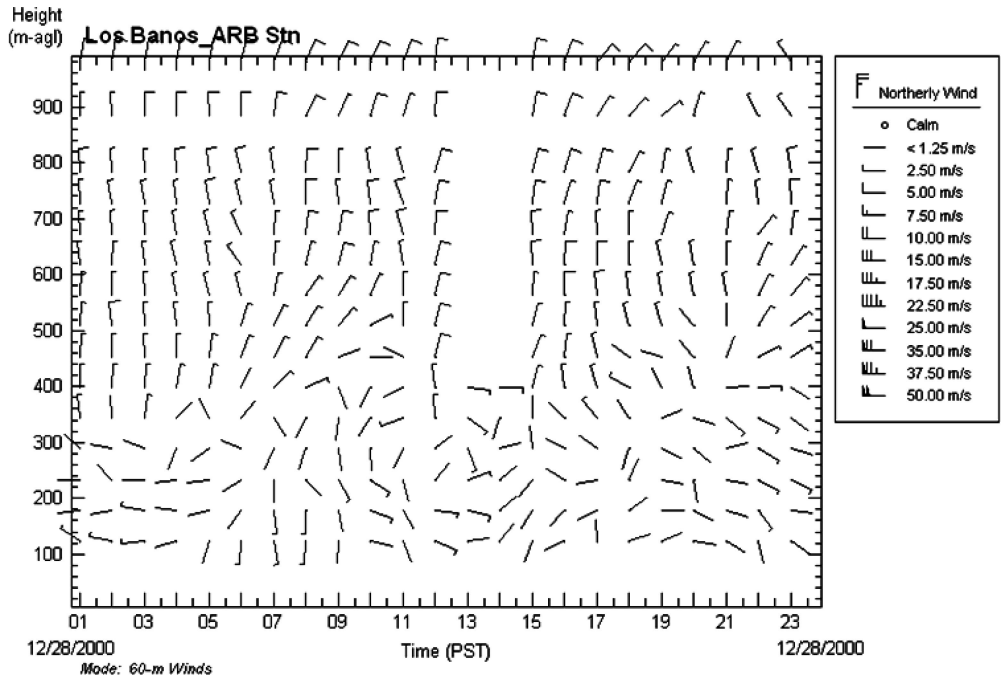

Figure 7. Los Banos RWP wind data on December 28, 2000.

Pass (ALT1); however, no evidence exists of transport from FSF or BAC out of the SJV through Paso Robles or Tehachapi Pass. This observation does not imply that pollutants did not exit the SJV via these passes, only that the pollutants did not originate in one of the major population centers in the SJV. Modeled trajectories for the two wintertime case studies yielded no evidence of transport from the SFBA to the SJV.

Modeled Dispersion. Dispersion modeling was performed for the case study periods. The emission range of influence and movement at each location in the SL was very similar in both case studies, except near the end of the January 2001 case study when a strong low-pressure system approached the West Coast. An example of dispersion output for the December and January episodes is shown in Figure 10. Table 1 summarizes the dispersion characteristics (plume size and movement) in and around the SJV throughout the January 2001 case study period. The size of the plume was estimated by measuring the distance from the population center to the contour that represented one tenth (5 $\mu g/m^3$) of the maximum modeled primary $PM_{2.5}$ concentration (50 $\mu g/m^3$). The highest concentrations and largest range of influence impacted by the emissions typically occurred overnight and in early morning hours, because low nighttime mixing

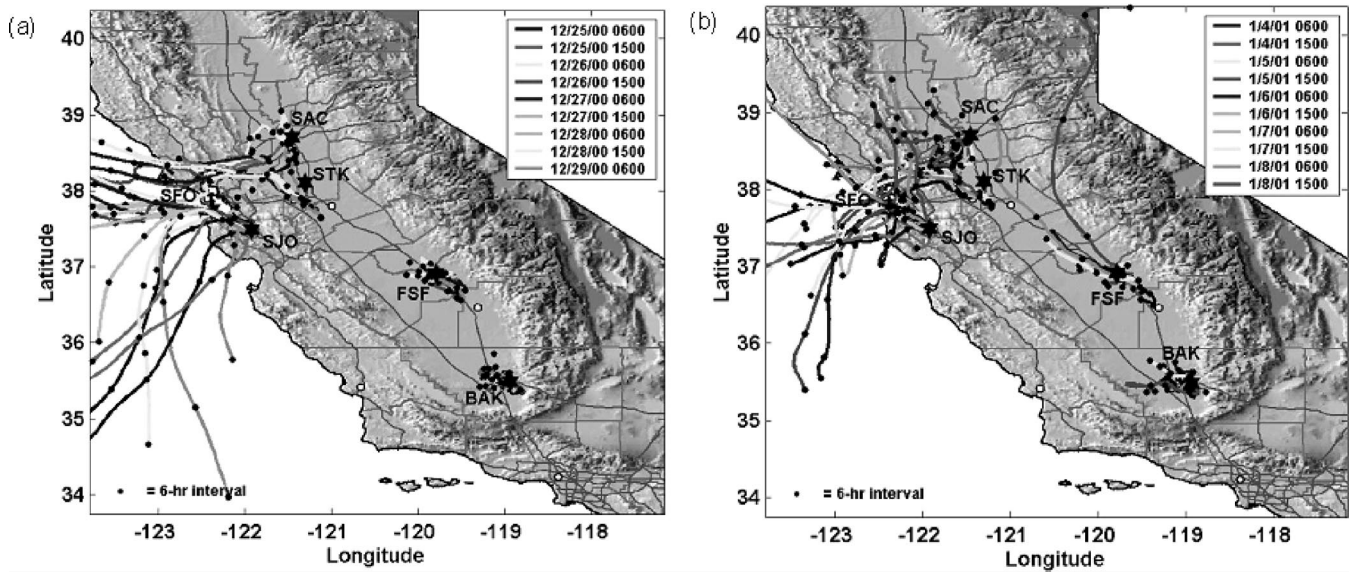

Figure 8. 24-hr forward trajectories initialized twice daily at 35 m agl from (a) December 25, 2000, at 6:00 a.m. PST through December 29, 2000, at 6:00 a.m. PST and (b) January 4, 2001, at 6:00 a.m. PST through January 8, 2001, at 3:00 p.m. PST.

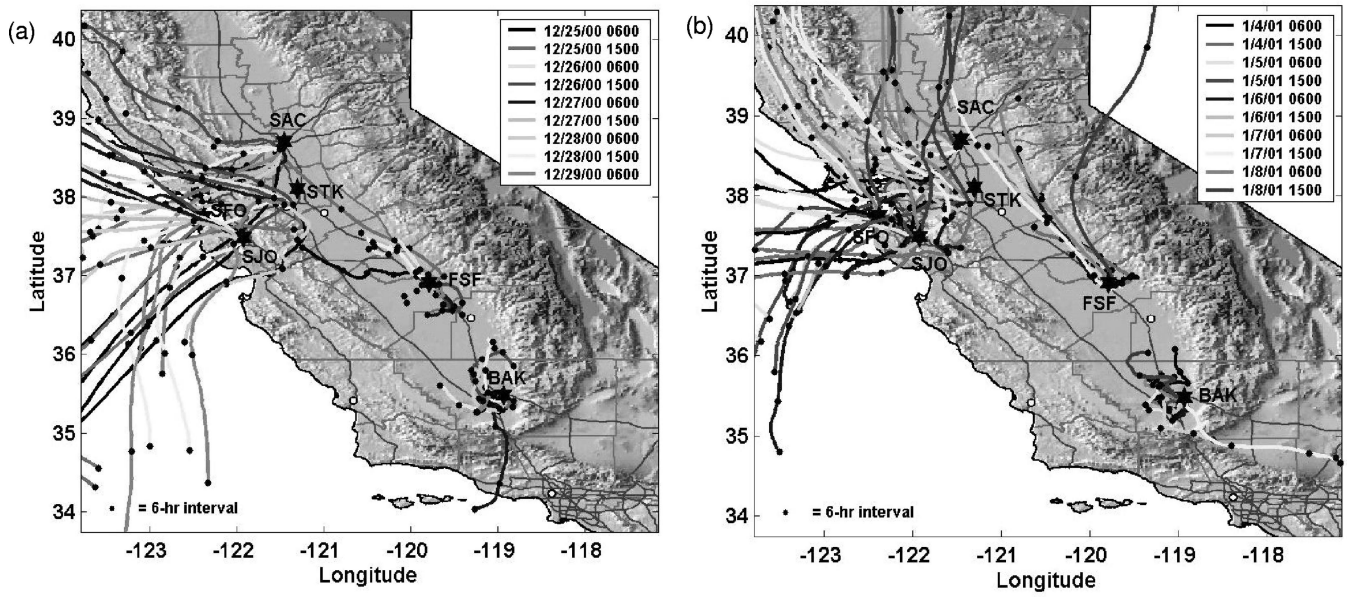

Figure 9. 24-hr forward trajectories initialized twice daily at 450 m agl from (a) December 25, 2000, at 6:00 a.m. PST through December 29, 2000, at 6:00 a.m. PST and (b) January 4, 2001, at 6:00 a.m. PST through January 8, 2001, at 3:00 p.m. PST.

heights limited the dispersion of the emissions. Despite continuous emissions and the model accumulation of pollutants throughout the simulation, the range of influence (as defined by one tenth of the maximum urban concentration) does not increase continuously throughout the period. The lack of increase occurs because the dispersion rate of pollutants, driven by increasing mixing height and wind speeds, is greater than the rate of accumulation.

Plumes from FSF and Sacramento subregions demonstrated the greatest range of influence and concentrations because of stronger boundary layer winds and higher emissions rates for both cities. For example, the mean range of the emission plume released from FSF was ~50 km compared with 25 km at BAC. The range of influence varied from 15 to 200 km for FSF, 15 to 100 km for Sacramento, and 15 to 30 km for BAC. The 200-km range of influence occurred at the end of the episode when southerly winds transported emissions to the east of Stockton and M14.

Ambient Concentration Spatial Analysis. OM was, on average, the second largest chemical component of $PM_{2.5}$ during the episode, although it was the largest component at a few urban sites. Figure 11 shows 24-hr average OM concentrations in the SJV during the winter 2000 and 2001 episode (December 14, 2000, to January 7, 2001). Particulate OM concentrations were high at the urban core sites and low at most rural sites. At distances >50 km

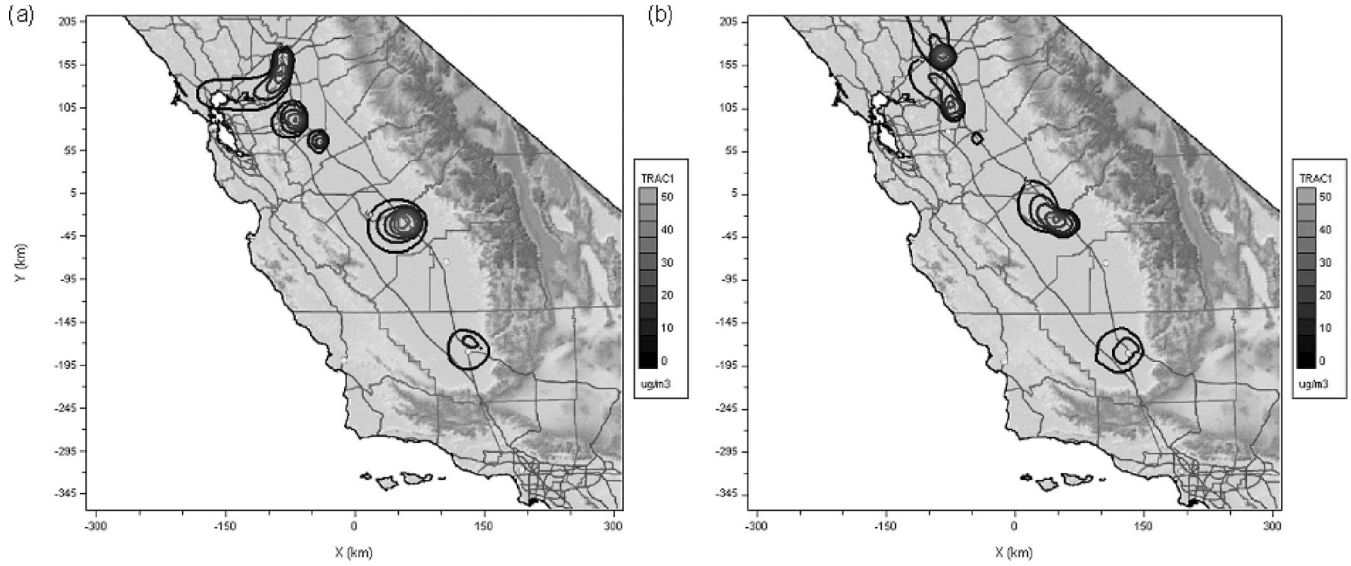

Figure 10. Surface concentration isopleths of CALPUFF simulated urban emissions for (a) December 27, 2000, at 6:00 a.m. PST and (b) January 6, 2001, at 6:00 a.m. PST.

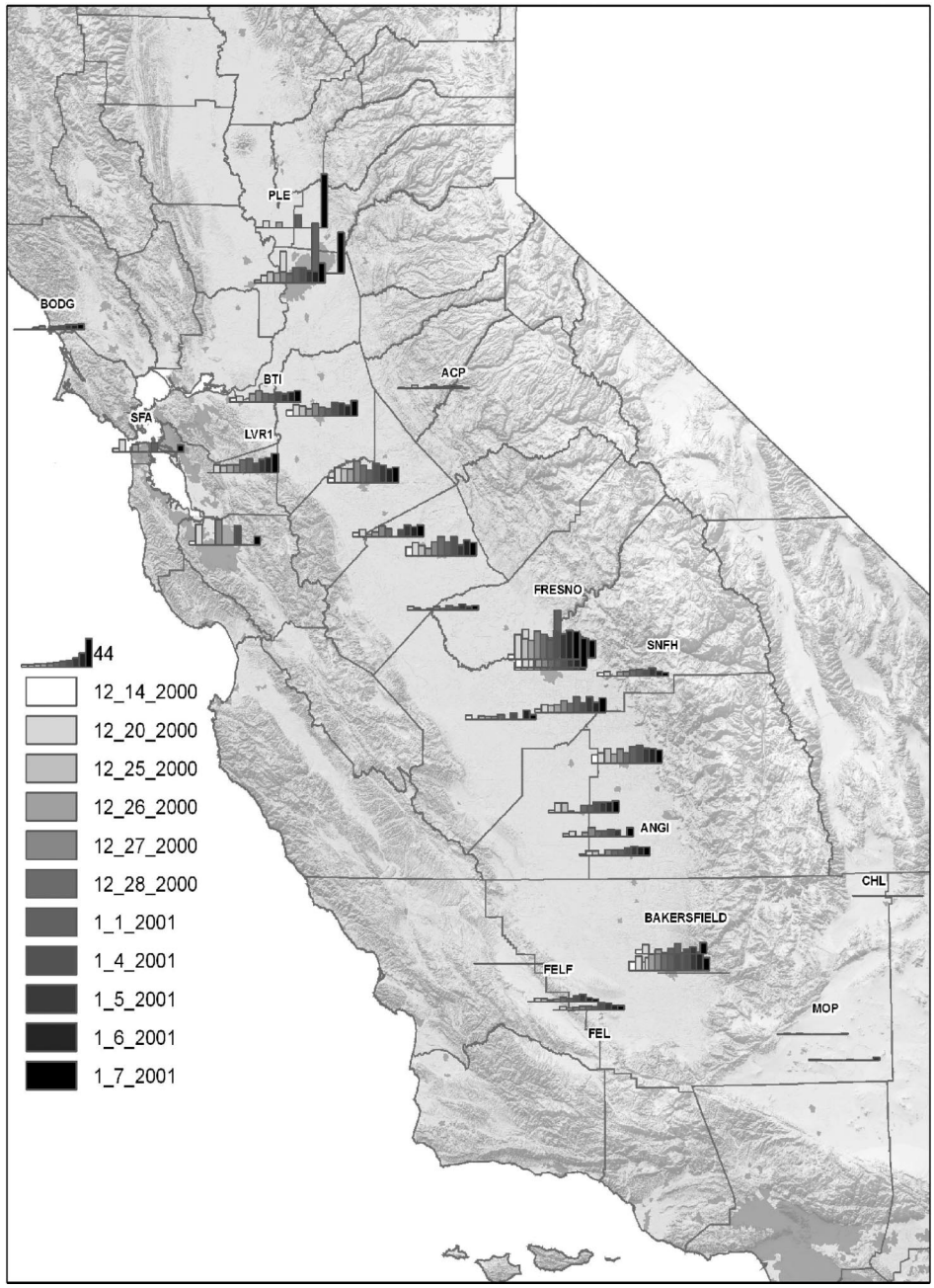

Figure 11. Particulate OM concentrations ($\mu g/m^3$) from December 14, 2000, through January 7, 2001, at CRPAQS monitoring sites. Note that measurements are not available or not shown for multiple days between December 14, 2000, and January 7, 2001.

from the urban areas, OM concentrations typically declined by a factor of 3–7. Concentrations of OM at elevated sites were comparable to concentrations at ruralsites on the valley floor. Possible positive and negative OC measurement artifacts caused by semivolatile adsorption and volatilization on the undenuded quartz filters were not large enough to account for the magnitude of urban/rural differences shown in Figure 11.[31–33] Overall, these spatial patterns of OM suggest that the impact of urban emissions was largely confined to the urban areas, and OM concentrations were unevenly distributed over the duration of the episode. Thus, modeled dispersion zones of influence of urban emissions are smaller than the observed spatial variability of OM observations. This difference can be explained by secondary OM formation, emissions from sources outside the urban area, and/or uncertainty in the model.

In contrast, ammonium nitrate can be classified as a regional pollutant, because it was relatively homogeneously distributed throughout the SJV; this homogeneity was evident on a smaller scale during IMS95.[10,34] Figure 12 shows the buildup of ammonium nitrate aerosol at all of the CRPAQS sites during the winter 2000 and 2001 episode (December 14, 2000, to January 7, 2001). Ammonium nitrate concentrations in the FSF and BAC urban areas were quite similar to concentrations at the ANGI and Helm rural sites. Ammonium nitrate concentrations at most rural sites were within a factor of 2 of the urban

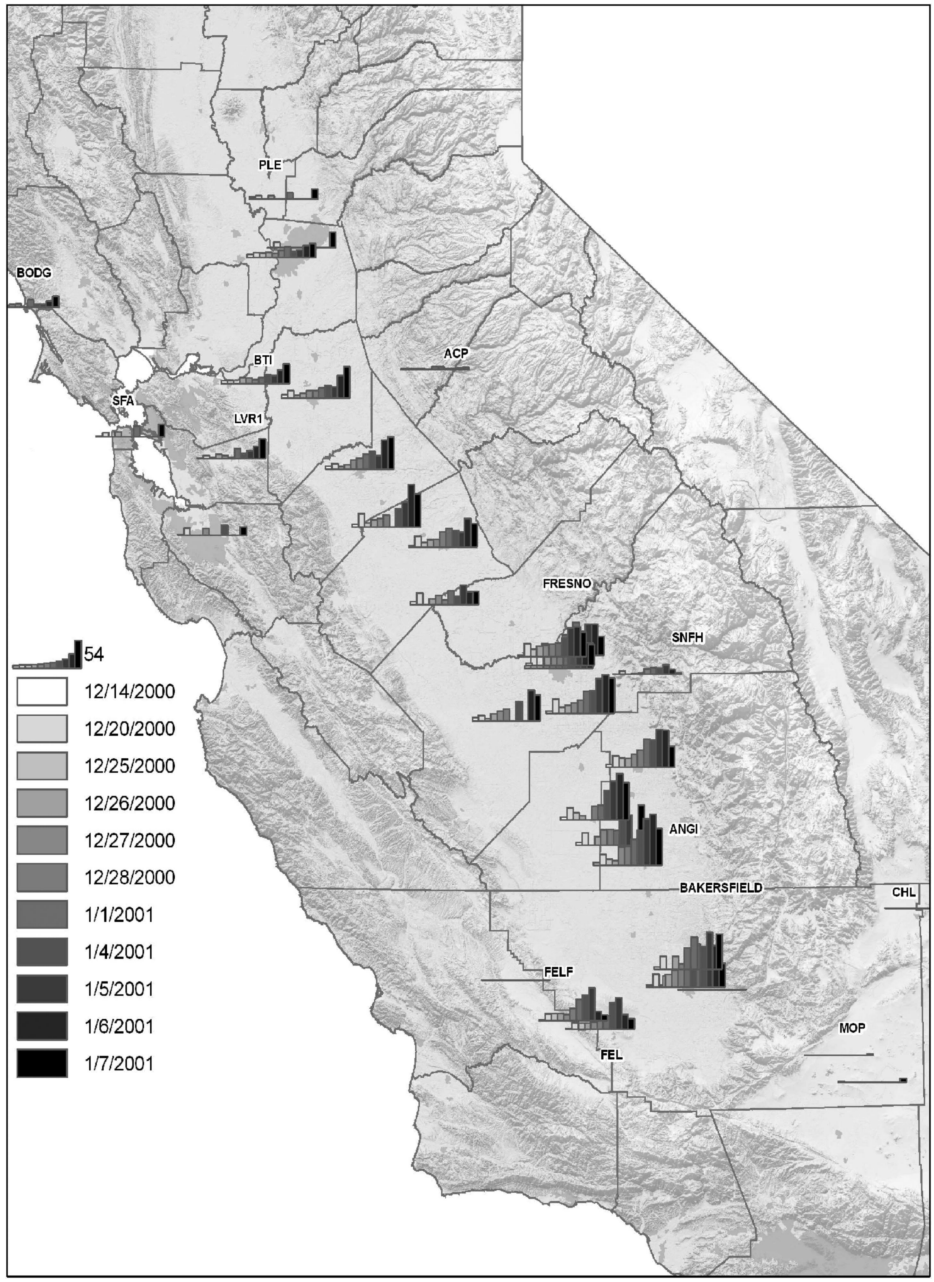

Figure 12. Particulate ammonium nitrate concentrations ($\mu g/m^3$) from December 14, 2000, through January 7, 2001, at CRPAQS monitoring sites. Note that measurements are not available or not shown for multiple days between December 14, 2000 and January 7, 2001.

sites and were temporally correlated with the urban sites. Ammonium nitrate concentrations were typically higher in the southern SJV than in the northern SJV or in the SFBA. Elevated sites, such as SNFH, ACP, and ALT1, measured significantly lower ammonium nitrate concentrations than urban or rural sites on the valley floor. This observed spatial pattern suggests that high concentrations of ammonium nitrate were essentially confined within the SJV by topography during this episode and is consistent with the low mixing heights estimated from RASS T_v data.

Pollution and Wind Roses at Interbasin Sites. PM and its precursors were not transported into the SJV in significant amounts during wintertime episodes. Wind rose plots for the western boundary site of ALT1 (37.76° N and 121.46° W), shown in Figure 13, indicate that the net flux of air was most frequently out of the SJV during winter episodes, which is consistent with the modeled wind trajectories shown in Figures 8 and 9. During the afternoon, when mixing heights are highest, wind flow was predominantly from the east; the average wind speed at these sites was <1 m/sec from the east. Pollution roses in Figure 13 show measurements of nephelometer light scattering because of particles (b_{sp}) plotted as a function of wind direction. Nephelometer measurements from the winter correlate with $PM_{2.5}$ concentrations in the SJV.[16,17,35] $PM_{2.5}$ concentrations were highest at the ALT1 site when the wind blew from the east. The nighttime and morning measurements for the ALT1 site show a higher frequency of winds blowing into the SJV, but the PM concentrations

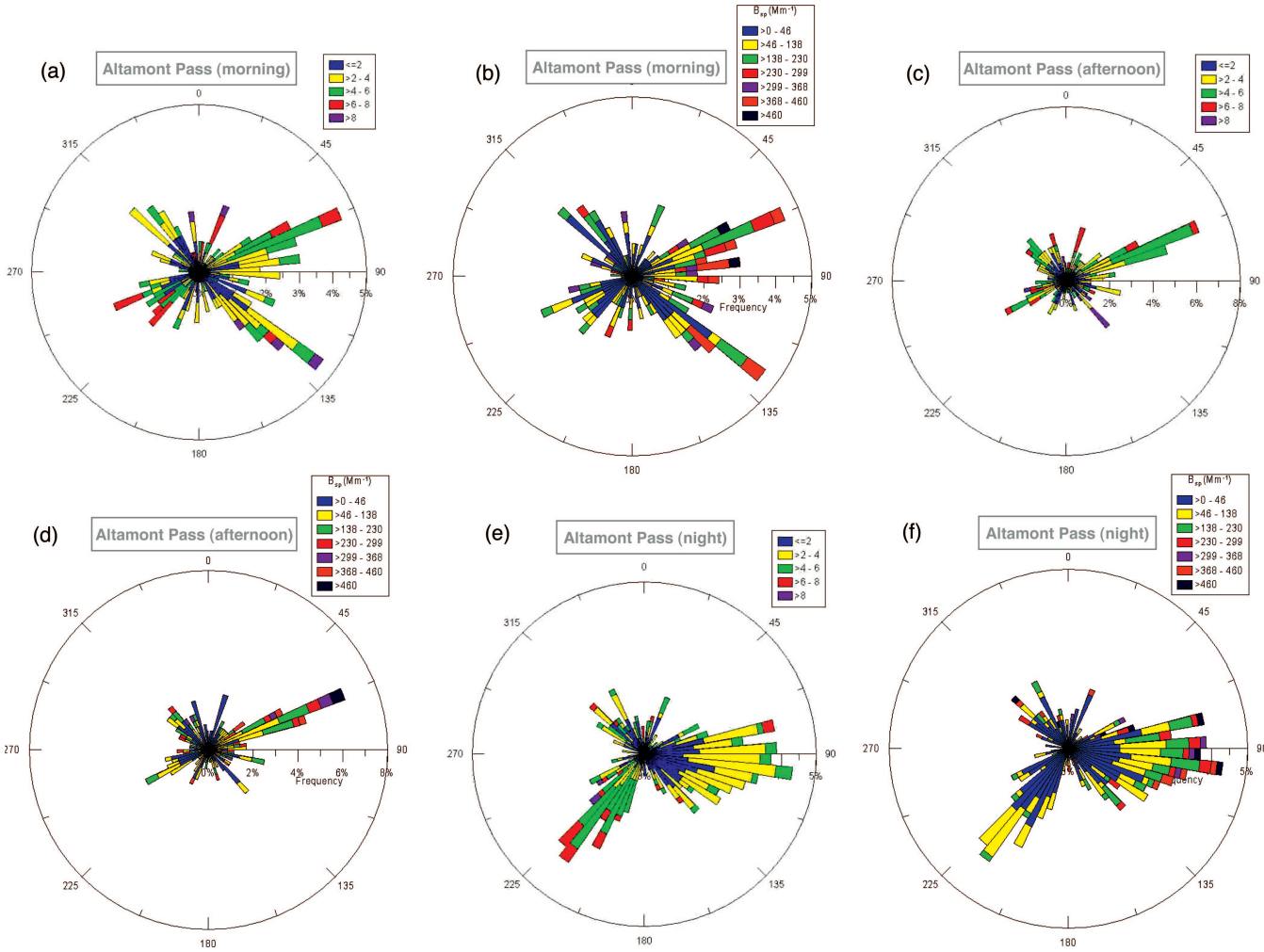

Figure 13. Wind (m/sec) and pollution roses from ALT1 during the winter episode from 6:00 a.m. to 11:00 a.m. PST (a and b), 12:00 p.m. to 5:00 p.m. PST (c and d), and 6:00 p.m. to 5:00 a.m. PST (e and f). Pollution roses plot the measured b_{sp} from the nephelometer and the direction from which the wind blew during the measurements; higher values correlate with higher PM concentrations.

associated with westerly winds are lower than those associated with easterly winds. Wind and pollution roses for the PAC1 site (data not shown) indicate similar patterns.

Wind roses at the eastern boundary site of King's River Valley (KRVM) indicate that the airflow was either upslope (west–northwest) or downslope (east–southeast). Wind data for the SNFH site show very similar patterns. The wind direction was directly aligned with the axis of the canyons to the east of the foothill sites. Upslope flow dominated during the afternoon; drainage flow occurred at night and in the mornings. The net flow was weak into the SJV from the foothills (<1 m/sec) during the winter. Pollution roses of nephelometer b_{sp} indicate that PM concentrations were low at KRVM during the winter. Pollution roses indicate that air flowing up the foothills in the afternoon turned around in the evening and flowed back down to the SJV during the evening drainage flow. Morning concentrations at the eastern boundary sites were more often representative of cleaner air (i.e., well below 10 $\mu g/m^3$). These inflow $PM_{2.5}$ concentrations were well below the concentrations typical of sites on the valley floor during episodes. Therefore, $PM_{2.5}$ concentrations from the Sierra Nevada Mountain sites transported to the SJV would dilute $PM_{2.5}$ concentrations on the valley floor.

DISCUSSION

Persistent synoptic-scale ridge or trough patterns correlated with PM episode and nonepisode days. Synoptic-scale ridge patterns suppressed mixing heights and wind speeds, leading to low ventilation index values. Persistent stagnation periods trapped emissions within the topographical confines of the SJV, leading to PM episodes. These synoptic-scale weather patterns can be used to identify high-PM days in the SJV.

Dispersion, trajectory, and spatial analyses provided evidence that little intrabasin interaction occurred among the SJV subregions. Dispersion and spatial analyses both showed that primary pollutants emitted in urban areas were unlikely to be transported in significant concentration much beyond 50 km in the MV and SV during PM episodes. For example, little, if any, interaction of simulated urban plumes appeared to occur between the FSF and BAC subregions.

The spatial analysis of ambient $PM_{2.5}$ OM and ammonium nitrate concentrations showed that secondary

formation mechanisms resulted in different spatial patterns than primary emissions. OM and ammonium nitrate were both subject to the same meteorological transport conditions (i.e., light surface, aloft winds, and low mixing heights) that should result in little transport away from urban areas as shown in the dispersion and trajectory analyses. The majority of the OM and ammonium nitrate component mass is a similar size fraction (PM with diameters of 0.1–1.0 μm),[36–38] and, therefore, the rates of removal should be approximately the same. Moreover, the distribution of the primary OM emissions and limiting NO_x ($NO + NO_2$) precursor[28] emissions were spatially concentrated near roadways and urban areas because of similar sources. Because the spatial distribution of emissions, removal rates, and meteorological transport are very similar for both OM and ammonium nitrate, the differences in spatial patterns are likely caused by the secondary formation mechanism of ammonium nitrate. The authors speculate that the formation of ammonium nitrate from NO_x precursors must occur at similar rates in both urban and rural areas in the SJV to account for its spatial homogeneity. This may be at least partially caused by aloft formation of ammonium nitrate[39–41] during the night, followed by entrainment of ammonium nitrate into the daytime boundary layer.

Dispersion, trajectory, and pollutant rose analyses showed evidence of interbasin transport from Sacramento through to the SFBA to offshore regions (Figures 8 and 9). Offshore flow through the ALT1 and Carquinez Straits from the NV may have contributed to PM concentrations in the SFBA. Additional analysis is necessary to determine whether the transport of pollutants into the SFBA was significant compared with local PM emissions. In contrast, transport of PM and precursors into the SJV from the Sierra Nevada Mountains was negligible during the winter study period; in fact, any transport from this area would reduce, not enhance, SJV PM concentrations.

CONCLUSIONS

To assess the spatial and temporal variability of transport and dispersion processes in the SJV impacting wintertime $PM_{2.5}$ concentrations, statistical analyses and case study analyses were performed. The case study analyses focused on meteorological modeling, dispersion modeling, trajectory analysis, spatial analysis, and wind and pollution roses.

Episode days occurred most often when persistent upper-level ridge patterns of high pressure suppressed mixing heights and boundary layer wind speeds. In contrast, upper-level trough patterns of low pressure increased wind speeds and helped ventilate the SJV, reducing PM concentrations.

Light boundary layer winds during episodes resulted in a calculated mean range of influence of 15–50 km for emissions from major cities in the SJV. This range of influence is defined as the maximum distance where concentrations are at least one tenth of the maximum modeled concentration. Dispersion analysis showed that simulated inert tracers emitted at either FSF and BAC did not impact one another. Moreover, spatial patterns of OM in the SJV showed large spatial variability, with high concentrations clustered near urban areas and low concentrations in rural areas. Finally, trajectory analysis illustrated that little intrabasin transport occurred among the north, central, and south SJV.

Interbasin transport was strongest in the NV subregion and Sacramento, with trajectories and pollutant roses showing transport across the delta and through mountain passes to the SFBA. In addition, dispersion analysis indicated that simulated tracers emitted in the NV subregion and Sacramento were transported into the SFBA. No evidence of transport from the SFBA into the SJV existed during these wintertime case studies. In addition, no evidence of strong nocturnal jets or eddy circulations significantly influencing transport in the SJV existed during the winter.

ACKNOWLEDGMENTS

This work was supported by the San Joaquin Valleywide Air Pollution Study Agency and managed by the California Air Resources Board (CARB). The authors gratefully acknowledge the assistance of Karen Magliano and Richard Hackney of the CARB.

The authors thank Mark A.R. Lilly for his efforts on this project including data processing, programming, data analysis, and creating plots for the analyses.

REFERENCES

1. Held, T.; Ying, Q.; Kaduwela, A.; Kleeman, M. Modeling Particulate Matter in the San Joaquin Valley with a Source-Oriented Externally Mixed Three-Dimensional Photochemical Grid Model; *Atmos. Environ.* **2004**, *38,* 3689-3711.
2. Watson, J.G.; Chow, J.C.A. Wintertime $PM_{2.5}$ Episode at the Fresno, CA, Supersite; *Atmos. Environ.* **2002**, *36,* 465-475.
3. Chow, J.C.; Watson, J.G.; Lowenthal, D.H.; Solomon, P.A.; Magliano, K.; Ziman, S.D.; Richards, L.W. PM_{10} and $PM_{2.5}$ Compositions in California's San Joaquin Valley; *Aerosol. Sci. Technol.* **1993**, *18,* 105-128.
4. Blumenthal, D.L.; Smith, T.B.; Lehrman, D.E.; Rasmussen, R.A.; Whitten, G.Z.; Baxter, R.A. *Southern San Joaquin Valley Ozone Study*; STI-94100-510-FR, Contract No. 84-8.0.05(2)-07-01; Sonoma Technology, Inc.: Santa Rosa, CA, 1985.
5. Roberts, P.T.; Smith, T.B.; Lindsey, C.G.; Lehrman, D.E.; Knuth, W.R. *Analysis of San Joaquin Valley Air Quality and Meteorology*; STI-98101-1006-FR; Sonoma Technology, Inc.: Santa Rosa, CA, 1990.
6. Smith, T.B.; Lehrman, D.E.; Reible, D.D.; Shair, F.H. *The Origin and Fate of Airborne Pollutants within the San Joaquin Valley*; California Institute of Technology and Meteorology Research, Inc.: Pasadena, CA, 1981.
7. Smith, T.B.; Lehrman, D.E.; Niccum, E.M.; Hackney, R. *SARMAP II Design: Analysis of the San Joaquin Valley Meteorological Environment during High PM_{10} Loading*; prepared by Technical & Business Systems, Inc.: Santa Rosa, CA, 1996.
8. Watson, J.G.; Gertler, A.W.; Prowell, G.H.; Chow, J.C.; Hering, S.V.; Richards, L.W.; Blumenthal, D.L. *Causes of Secondary Aerosol in the San Joaquin Valley Determined from the WOGA Aerosol Data Base*; DRI Document No. 6687.4F1; Desert Research Institute: Reno, NV, 1987.
9. Main, H.H.; Richards, L.W.; Hurwitt, S.B.; Chinkin, L.R. *Characterization of the Spatial and Temporal Patterns of Visibility in the San Joaquin Valley during IMS95*; STI-997217-1778-FR; Sonoma Technology, Inc.: Petaluma, CA, 1998.
10. Kumar, N.; Lurmann, F.W.; Pandis, S.; Ansari, A. *Analysis of Atmospheric Chemistry during 1995 Integrated Monitoring Study*; STI-997214-1791-FR; Sonoma Technology, Inc.: Petaluma, CA, 1998.
11. Hayes, T.P.; Kinney, J.J.R.; Wheeler, N.J.M. *California Surface Wind Climatology*; prepared by the California Air Resources Board, Aerometric Data Division, Meteorology Section: Sacramento, CA, 1984.
12. Carroll, J.J.; Baskett, R.L. Dependence of Air Quality in a Remote Location on Local and Mesoscale Transports: A Case Study. *J. Appl. Meteorol.* **1979**, *18,* 4.
13. Roberts, P.T.; Main, H.H. *The Measurement of Pollutant and Meteorological Boundary Conditions: Technical Support Study Number* 10; STI-98030-920-FR; Sonoma Technology, Inc.: Santa Rosa, CA, 1989.

14. Blumenthal, D.L.; Lurmann, F.W.; Roberts, P.T.; Main, H.H.; MacDonald, C.P.; Knuth, W.R.; Niccum, E.M. *Three-Dimensional Distribution and Transport Analyses for SJVAQS/AUSPEX*; STI-91060-1705-FR; Sonoma Technology, Inc.: Santa Rosa, CA; Technical & Business Systems: Santa Rosa, CA; and California Air Resources Board: Sacramento, CA, 1997.
15. Pun, B.K.; Seigneur, C. Understanding Particulate Matter Formation in the California San Joaquin Valley: Conceptual Model and Data Needs; *Atmos. Environ.* **1999**, *33,* 4865-4875.
16. Richards, L.W.; Alcorn, S.H.; McDade, C.; Couture, T.; Lowenthal, D.; Chow, J.C.; Watson, J.G. Optical Properties of the San Joaquin Valley Aerosol Collected during the 1995 Integrated Monitoring Study; *Atmos. Environ.* **1999**, *33,* 4787-4795.
17. Alcorn, S.H.; Richards, L.W.; Lehrman, D. *Comparisons between Light Scattering and Fine-Particle Mass Data. California Regional $PM_{10}/PM_{2.5}$ Air Quality Study (CRPAQS) Task 1.1a*; STI-902321-2644, Sonoma Technology, Inc.: Petaluma, CA, 2004.
18. Motallebi, N.; Taylor, C.A.; Croes, B.E. Particulate Matter in California: Part 2—Spatial, Temporal, and Compositional Patterns of $PM_{2.5}$, $PM_{10-2.5}$, and PM_{10}. *J. Air & Waste Manag. Assoc.* **2003**, *53,* 1517-1530.
19. Scire, J.S.; Robe, F.R.; Fernau, M.E.; Yamartino, R.J. *A User's Guide for the CALMET Meteorological Model (Version* 5); Earth Tech: Concord, MA, 2000.
20. Scire, J.S.; Strimaitis, D.G.; Yamartino, R.J. *User's Guide for the CALPUFF Dispersion Model*; No. 1406-02; EARTH TECH/Sigma Research Corp.: Concord, MA, 1995.
21. Black, T.L. The New NMC Mesoscale Eta Model: Description and Forecast Examples; *Weather Forecast.* **1994**, *9,* 265-278.
22. Rogers, E.; Baldwin, M.; Black, T.; Brill, K.; Chen, F.; DiMego, G.; Gerrity, J.; Manikin, G.; Mesinger, F.; Mitchell, K.; Parrish, D.; Zhao, Q. *Changes to the NCEP Operational "Early" Eta Analysis/Forecast System*; No. 447; prepared by National Weather Service, Office of Meteorology: Silver Spring, MD, 1997.
23. California Air Resources Board. Almanac Emission Projection Data; available at: *http://www.arb.ca.gov/ei/maps/statemap/cntymap.htm* (accessed 2006).
24. Stull, R.B. *An Introduction to Boundary Layer Meteorology*; Kluwer Academic Publishers: Norwell, MA, 1988.
25. Garratt, J.R. *The Atmospheric Boundary Layer*; Cambridge University Press: Cambridge, UK, 1992.
26. Holzworth, G.C. Estimates of Mean Maximum Mixing Depths in the Contiguous United States; *Mon. Wea. Rev.* **1964**, *92,* 235-242.
27. Holzworth, G. *Mixing Heights, Wind Speeds, and Potential for Urban Air Pollution throughout the Contiguous United States*; Publication No. AP-101; Prepared by the Office of Air Programs, U.S. Environmental Protection Agency: Research Triangle Park, NC, 1972.
28. Lurmann, F.W.; Brown, S.G.; McCarthy, M.C.; Roberts, P.T. Processes Influencing Secondary Aerosol Formation in the San Joaquin Valley during Winter; submitted.
29. California Air Resources Board. California Air Basin Map; available at: *http://www.arb.ca.gov/ei/maps/statemap/abmap.htm* (accessed 2006).
30. Lorenzen, A., ed. *Summary of California Upper Air Meteorological Data*; prepared by the California Air Resources Board, Technical Services Division: CA, 1979.
31. Mader, B.T.; Pankow, J.F. Study of the Effects of Particle-Phase Carbon on the Gas/Particle Partitioning of Sernivolatile Organic Compounds in the Atmosphere Using Controlled Field Experiments; *Environ. Sci. Technol.* **2002**, *36,* 5218-5228.
32. Watson, J.G.; Chow, J.C. Comparison and Evaluation of in Situ and Filter Carbon Measurements at the Fresno Supersite; *J. Geophys. Res.* **2002**, *107*.
33. Subramanian, R.; Khlystov, A.Y.; Cabada, J.C.; Robinson, A.L. Positive and Negative Artifacts in Particulate Organic Carbon Measurements with Denuded and Undenuded Sampler Configurations; *Aerosol Sci. Technol.* **2004**, *38,* 27-48.
34. Magliano, K.L.; Hughes, V.M.; Chinkin, L.R.; Coe, D.L.; Haste, T.L.; Kumar, N.; Lurmann, F.W. Spatial and Temporal Variations in PM_{10} and $PM_{2.5}$ Source Contributions and Comparison to Emissions during the 1995 Integrated Monitoring Study; *Atmos. Environ.* **1999**, *33,* 4757-4774.
35. Chow, J.C.; Watson, J.G.; Lowenthal, D.H.; Richards, L.W. Comparability between $PM_{2.5}$ and Light Scattering Measurements; *Environ. Monit. Assess.* **2002**, *79,* 29-45.
36. Lighty, J.S.; Veranth, J.M.; Sarofim, A.F. Combustion Aerosols: Factors Governing Their Size and Composition and Implications to Human Health; *J. Air & Waste Manage. Assoc.* **2000**, *50,* 1565-1618.
37. Hughes, L.S.; Allen, J.O.; Kleeman, M.J.; Johnson, R.J.; Cass, G.R.; Gross, D.S.; Gard, E.E.; Galli, M.E.; Morrical, G.D.; Fergenson, D.P.; Dienes, T.; Noble, C.A.; Liu, D.-Y.; Silva, P.J.; Prather, K.A. Size and Composition Distribution of Atmospheric Particles in Southern California; *Environ. Sci. Technol.* **1999**, *33,* 3506-3515.
38. Bench, G.; Grant, P.G.; Ueda, D.; Cliff, S.S.; Perry, K.D.; Cahill, T.A. The Use of STIM and PESA to Measure Profiles of Aerosol Mass and Hydrogen Content, Respectively, across Mylar Rotating Drums Impactor Samples; *Aerosol. Sci. Technol.* **2002**, *36,* 642-651.
39. Geyer, A.; Stutz, J. Vertical Profiles of NO_3, N_2O_5, O_3, and NO_x in the Nocturnal Boundary Layer: 2. Model Studies on the Altitude Dependence of Composition and Chemistry; *J. Geophys. Res.* **2004**, 10.1029/2003JD004211.
40. Stutz, J.; Alicke, B.; Ackermann, R.; Geyer, A. Vertical Profiles of NO_3, N_2O_5, O_3, and NO_x in the Noctural Boundary Layer: 1. Observations during the Texas Air Quality Study 2000; *J. Geophys. Res.* **2004**, 10.1029/2003JD004209.
41. Neuman, J.A.; Nowak, J.B.; Brock, C.A.; Trainer, M.; Fehenseld, F.C.; Holloway, J.S.; Hubler, G.; Hudson, P.K.; Murphy, D.M.; Hicks, D.K., Jr.; Orsini, D.; Parrish, D.D.; Ryerson, T.B.; Sueper, D.T.; Sullivan, A.; Weber, R. Variability in Ammonium Nitrate Formation and Nitric Acid Depletion with Altitude and Location over California; *J. Geophys. Res.* **2003**, *108,* 4557.

About the Authors

Clinton P. MacDonald is manager of meteorological and air quality analysis services, Michael C. McCarthy is an air quality analyst, Paul T. Roberts is the executive vice president, air quality and exposure studies; Timothy S. Dye is vice president, meteorological programs and public outreach; and Neil J.M. Wheeler is vice president, atmospheric modeling and information systems, at Sonoma Technology, Inc. Address correspondence to: Clinton P. MacDonald, Sonoma Technology, Inc., 1360 Redwood Way, Suite C, Petaluma, CA 94954; phone: +1-707-665-9900; fax +1-707-665-9800; e-mail: clint@sonomatech.com.